Appendix

Chapter 3: Planthopper bugs use a fast, cyclic elastic recoil mechanism for effective vibrational communication at small body size

Leonidas-Romanos Davranoglou[1], Alice Cicirello[2], Graham K. Taylor[1], Beth Mortimer[1]

[1]Department of Zoology, University of Oxford, Oxford, OX1 3PS, U.K.;

[2]Department of Department of Engineering Science, University of Oxford, Oxford, OX1 3PJ, U.K.

Supplementary material

S1 Methods (link)

Insects

Larvae of *Agalmatium bilobum* were collected on *Asphodelus fistulosus*, whereas adults were collected from a variety of other plants. Larvae were reared with their potted host plant or daffodils (*Narcissus pseudonarcissus*). Many adults exhibited wing deformities from improper moulting, indicating that humidity levels were not optimal. Such individuals were excluded from our study. Adults were separated from each other as soon as they moulted and placed in unisex meshed cages.

Morphological analysis

To investigate the presence of resilin in the snapping organ of *A. bilobum* (S1 Fig), the thorax and the first three abdominal segments were dissected from five chilled individuals (0 oC for 5 minutes). The dissected snapping organs were immediately placed in excavated microscope slides and viewed through a Leica DM2000 LED under ultraviolet (UV) illumination at 365 nm, using a general blue (465/20)/green (530/30)/red (640/40) bandpass

filter and a MC120 HD camera. Images captured at the same focal planes under UV and visible light were superimposed using Photoshop CS6.

Power calculations

The mid-abdomen recordings taken orthogonal to the thorax were analysed to extract the co-ordinates of the maximum and minimum velocities of the loading and unloading steps and the last x axis crossing before the absolute maximum peak (S1 Data). The peak kinetic energy of the motion was calculated from the speed of the measured dorsoventral translation of the abdominal mass, multiplying its square by 0.5 times the abdomen mass (10.33 mg). For mass estimation, the abdomen of a single female adult *A. bilobum* was excised and measured in a Sartorius CPA225D semi-micro balance.

To calculate the power, the energy was divided by the time taken to reach peak velocity from rest. To calculate the power and energy density, muscle mass was required. We assumed a muscle density of 1060 kg m-3 and measured muscle lengths and diameters from the micro-CT data (one female *A. bilobum*), estimating muscle volumes by approximating them as cylinders. We calculated the maximum muscle mass, which was the pair of DLMs (Idlm1, Idlm2) added to the smaller paired DVM muscles (IIedvm1, IIedvm2, Fig 2, S1 Data). Power density was then calculated as the power divided by paired muscle mass from all four muscles. Energy density was the energy divided by the paired DLM muscle mass for both DLMs.

Mathematical model

Available here.

S1 Text (link)

Extended description of the snapping organ of *Agalmatium bilobum* (Issidae)

1. Exoskeleton

The morphology of the first and second abdominal segments is complex. A narrow, sclerotized strip fused to the metapostnotum and metepimeron represents the anterior-most part of the first abdominal tergum (Figs 1B, 2A, yellow). This strip bears the first abdominal spiracle, a pair of arm-like ridges (Fig 1B, rg), and is ventrally continuous with the postcoxale (formed by the first abdominal segment; Fig 2A, yellow). The opposing ridges fuse dorsally (Fig 1B) on the anterior arm of a modified, Y-shaped lobe of tergum one (Figs 1B, rg, 2A, brown). A distinctive seta is present in the dorsal portion of each ridge (not shown). The sclerotized metapostnotal strip and the Y-lobe are separated by a folded membrane (Fig 1B). The anterior arm of the Y-lobe is continuous dorsally, while its posterior arm fuses to tergum two (Fig 1B, tg 2) and dorsomedially terminates adjacent to a pair of apodemes of segment two (S1 Fig, Fig 2B, apo), which serve as attachments for the hypertrophied Idlm1 muscles (Fig 2B, apo). The two arms of the Y-lobe are separated by a membrane containing resilin, separated from each other at the midline by a segment of cuticle (S1 Fig). Tergum two is subdivided into a proximal sclerotized portion (Fig 1B, green) and a distal membranous, cushion-like pad. The lateral margin of the sclerotized portion of tergum two bears posteriorly a pair of connector arms, which link it to tergum three. The spiracle of the second abdominal segment is fused to tergum two, forming the proximal portion of the segments' lateral margin (Fig 1B). The lateral margin of tergum two is crescent-shaped, distinctly separating the fused lobe of the second abdominal spiracle and the connector arms (Figs 1B, 2A). Immediately beneath spiracle two, a small orifice forms internally a downward-facing spine (Fig 2C, sp). A connective from the base of the Y-lobe fuses to this spine-like apodeme, linking the two segments functionally and morphologically (Figs 1B, cn, 2A).

Both segments are characterized by subdivided sternites one and two (Fig 2A). The anterior and posterior margins of each sternite are sclerotized, while their median region is divided by a broad membrane. The first subdivision of sternum one (stnIa) is fused to the metafurca and forms the postcoxale (Fig 2A, yellow), while the second (stnIb) is represented by a short sclerotized flap, immediately anterior to sternum two. stnIIa and stnIIb are interrupted by a membrane, like the previous segment and are also strip-like. A small apodeme protrudes from the median region of stnIIa (not shown), while stnIIb is closely associated with segment three both dorsally and ventrally. Both subdivisions of the second segment terminate into a spatulate apex (Fig 2A).

2. Musculature and nervous system

The segmental affinities of the dorsoventral muscles and ventral sclerites operating the snapping organ and the tymbal-like organs of Cicadomorpha have been contentious, with some authors assigning them to the first abdominal segment [1, 2] and others to the second [3, 4]. Based on innervation as observed by SR-µCT (S2 Fig), the primary dorsoventral muscles attaching on the internal spine of the second abdominal tergum (Fig 2A, C) are innervated by the second abdominal nerve (S2 Fig, n.ab. 2) and belong to the second abdominal segment. The two main dorsal longitudinal muscles – the hypertrophied Idlm1 and the smaller Idlm2 (Fig 2A), are innervated by the first abdominal nerve (S2 Fig, n.ab. 1) and belong to the corresponding segment. A summary of the origins and insertions of all muscles involved in the snapping organ, together with their inferred functions, is provided in S2 Table.

The snapping organ in other planthopper families

The exoskeletal components defining the snapping organ of our model species, *A. bilobum*, i.e. the characteristic arrangement of the ridge, Y-lobe and connector, were found in all 21

examined planthopper families (S1 Table). Although the overall morphology and arrangement of the snapping organ exoskeleton is remarkably constant, there is some variation in the general shape of its components (Figs 2, 3), with the main variants described below:

1) The **ridge** in all examined taxa acts as a bridge between the first abdominal segment strip (fused to the metapostnotum) and the anterior Y-lobe arm. However, it may cover only a small portion of the anterior Y-lobe arm (e.g. in some Cixiidae and Asiracinae, Fig 3B, C), or completely envelop it and fuse with the ridge on the other side of the organ (e.g. Caliscelidae, Fig 2E, tettigometrids). The distinct seta on each ridge is invariably present in all examined planthoppers.

2) The **Y-lobe** is typically Y-shaped, with anterior and posterior arms, connecting to the ridge and tergite two respectively. The Y-lobe base may vary significantly in shape, ranging from short and robust (e.g. cixiids, Fig 3B), to elongate (most planthoppers, Figs 1B, 3C, D). In addition, the Y-lobe may be entirely transparent in small, soft bodied forms (e.g. many Meenoplidae, Kinnaridae and Issidae). A characteristic shared by all examined Dictyopharidae and Fulgoridae, is that the posterior arm of the Y-lobe and the apodemes of Idlm1 on tergite two are not visible externally.

3) The **connector** always links the base of the Y-lobe to the base of tergite two. The connector may be entirely membranous in some taxa (e.g. some Issidae), or considerably sclerotized (e.g. tettigometrids). Its shape may vary from very narrow (e.g. Issidae, Figs 1B, 2) to quite broad (e.g. Flatidae, Nogodinidae, Ricaniidae).

4) **Tergite two** is generally quite uniform. The median incision between the apodemes for Idlm1 may be shallow (many Issidae, Flatidae, Caliscelidae, Lophopidae etc.), extending to more than half of the tergite length (e.g. Fig 3B, C, D), or completely absent (many

Dictyopharidae and Fulgoridae). Tergite two may be distinctly subdivided into an anterior sclerotized part and a posterior membranous region (Fig 1). The membranous region may be very small (Fig 3B, C), interrupted by a median sclerotized region (Fig 3D), or entirely absent (Fig 3E). The anterior sclerotized region may frequently be raised, strongly convex (e.g. most ricaniids, flatids, nogodinids), slightly less raised (e.g. most eurybrachids) or almost entirely flat (e.g. most Issidae, Fig 1B).

We have not observed sexual dimorphism in the morphology of the snapping organ in any of the examined species (S1 Table).

All the above exoskeletal variations can be found in various combinations throughout planthoppers, which suggests that these variations have arisen many times independently. The musculature defining the snapping organ is even more uniform in 11 of the 12 families examined using SR-μCT (S1 Table), consistent with a single origin at the base of fulgoromorphan phylogeny (Fig 3). The examined non-cedusine derbids are an exception, in which the Y-lobe is externally obscure (S3 Table), and is supplemented by a tentative wing stridulatory mechanism.

The subtle variations in the external morphology of the snapping organ beyond the given defining characters between planthopper families are likely to be of significant systematic and taxonomic importance, and more detailed studies are necessary. The modified organs of delphacids are species-specific and already used in both taxonomic and systematic studies [3, 5]; we expect that the same holds true for the remaining planthoppers.

Overall, the defining exoskeletal elements and muscles of the snapping organ are constant across the examined planthopper taxa (with the exception of some delphacids, Fig 2; see below). The above suggest that the vibrational mechanism is also conserved, which is supported by the overall uniformity in signal structure of most planthoppers [6, 7]. Given

that the earliest definitive planthoppers originated in the Jurassic (260 million years ago) [8, 9], the snapping organ represents a remarkably conserved bauplan. However, it is possible that additional, as yet undiscovered components or vibration generation mechanisms may also supplement the calls of planthoppers possessing a snapping organ.

The delphacid "drumming organ"

The vibrational organ (also known as drumming organ) of non-asiracine delphacids has long been thought to represent the mechanism of vibration generation of planthoppers as a whole [3, 5, 6, 10]. In contrast, we suggest that the drumming organ of delphacids is a modified snapping organ, sharing the same bauplan: A series of cumulative exoskeletal and muscle transformations (S3 Table) [5] in non-Asiracinae Delphacidae has led to the development of a very specialized structure, which presumably functions differently from the snapping organs of other planthoppers. Although the defining characteristics of the snapping organ are present, the vibrational organs of non-Asiracinae have undergone such drastic reorganization and addition of novel components, such as the central plate (S3A Fig), which makes it unlikely that they function in the same way as snapping organs. Given that the homologies of the vibrational organs of planthoppers and non-Asiracinae have never been elucidated, we briefly describe below our interpretations of the exoskeleton and musculature of the delphacid drumming organ.

We describe the exoskeletal components of the drumming organ in a generalized delphacid – *Stenocranus minutus*, which would be applicable for most non-Asiracinae delphacids. The metapostonotal apodemes are centrally located, and strongly expanded ventrally (S3 Table). Each ridge is greatly expanded, spatulate in shape (S3A, B, C Fig, yellow). The distinctive seta found on the ridge of other planthoppers is present, but located towards the base of the ridge. The two opposing ridges are separated by a transparent cuticular bridge of uncertain

origin (S3A, B, C Fig, pink) – it may represent an unmodified section of tergite one, or an expansion of the anterior Y-lobe arm. The entire Y-lobe is strongly reduced to a small rounded lobe, fused to the posterior lateral margin of each ridge (S3A, B, C Fig, lb, brown). The Y-lobe rudiment bears a transverse list, of uncertain function (S3C Fig, lt). Due to the rudimentary and modified nature of the Y-lobe in non-Asiracinae delphacids, we cannot ascertain whether the posterior Y-lobe arm is either strongly reduced or completely absent. The entire median region of tergite two has been transformed into a central plate (S3A, B Fig, cp) which internally supports large apodemes for the greatly enlarged Idlm1 (S3B Fig).

We examined the musculature of the drumming organ of delphacids by using SR-μCT in *S. minutus* and compared them with illustrations from previous morphological studies [3-5] and SR-μCT scans of planthoppers from the other 11 planthopper families (S1 Table). We observed that the drumming organs (i.e. the modified snapping organs of non-Asiracinae delphacids) use the same musculature with the rest of Fulgoromorpha (S3D Fig, S3, S4 Tables), although their relative size (and probably function as well) is different. In non-Asiracinae delphacids, exemplified here by *S. minutus*, there is a general trend for enlargement of the dorsoventral and longitudinal musculature of the first two abdominal segments: muscles that are small (IIIvlm3, IIvlm2, IIedvm1) or thread-like (e.g. IIidvm1) in most Fulgoromorpha are greatly enlarged in non-Asiracinae delphacids (S3D Fig). Muscle Idlm1, which is already hypertrophied in all examined planthoppers, is even larger in non-Asiracinae delphacids [3, 4]. In addition, the downward expansion of the metapostnotal apodemes, have provided this muscle with a near-dorsoventral position, with possible functional implications. We found muscle Idvm in *S. minutus*, which has not been reported previously from delphacids (S3D Fig, S4 Table), while we could not locate IIidvm2. There may be variation in the size of the different dorsoventral muscles in different delphacid taxa;

in *S. minutus*, II edvm1 is the largest dorsoventral muscle, whereas in *Nilaparvata lugens*, IIidvm1 is the largest [4].

References

1. Snodgrass RE. Morphology of the insect abdomen. 1. General structure of the abdomen and its appendages. Smith Misc Coll. 1931; 85: 1-128.

2. Kramer S. The morphology and phylogeny of auchenorrhynchous Homoptera (Insecta). Urbana-Champagne: University of Illinois Press; 1950.

3. Ossiannilsson F. Insect drummers. A study on the morphology and function of the sound-producing organ of swedish Homoptera Auchenorrhyncha. Op Ent Suppl 10. 1949; 3: 1-146.

4. Mitomi M, Ichikawa T & Okamoto H. Morphology of the vibration-producing organ in adult rice brown planthopper, *Nilaparvata lugens* (Stal) (Homoptera: Delphacidae). Appl Entomol Zool. 1984; 19: 407-417.

5. Asche M. Vizcayinae, a new subfamily of Delphacidae with revision of *Vizcayia* Muir (Homoptera: Fulgoroidea) - a signficiant phylogenetic link. Bishop Mus Occ Papers. 1990; 30: 154-187.

6. Tishechkin DY. On the similarity of temporal pattern of vibrational calling signals in different species of Fulgoroidea (Homoptera: Auchenorrhyncha). Russ Entomol J. 2008; 17: 349-357.

7. Tishechkin DY. On the similarity of temporal pattern of vibrational calling signals in different species of Fulgoroidea (Homoptera: Auchenorrhyncha). Russ Entomol J. 2008; 17: 349-357.

8. Song N & Liang AP. A Preliminary Molecular Phylogeny of Planthoppers (Hemiptera: Fulgoroidea) Based on Nuclear and Mitochondrial DNA Sequences. PLoS ONE. 2013; 8: e58400.

9. Urban JM & Cryan JR. Evolution of the planthoppers (Insecta: Hemiptera: Fulgoroidea). Mol Phyl Evol. 2007; 42: 556-572.

10. Wessel A, Mühlethaler R, Hartung V, Kustor V & Gogala M. The tymbal: evolution of a complex vibration-producing organ in the Tymbalia (Hemiptera excl. Sternorrhyncha). In: Cocroft RB, Gogala M, Hill PSM & Wessel A, editors. Animal signals and communication: studying vibrational communication. Berlin: Springer; 2014. pp. 395-444.

S1 Figures (link in each figure legend)

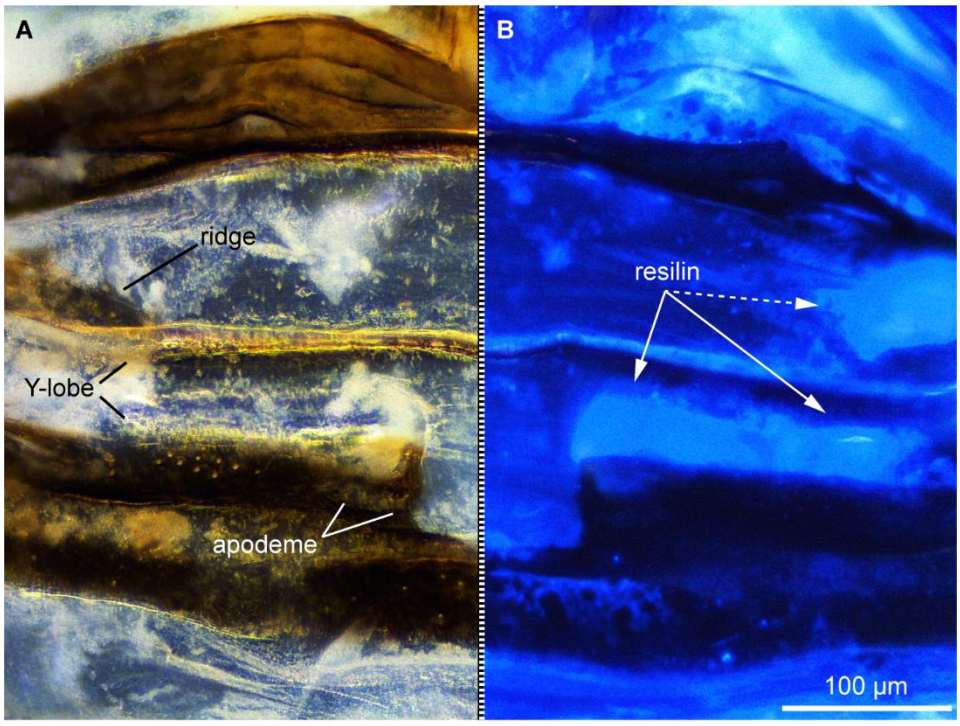

S1 Fig. Dissected snapping organ of a male *A. bilobum*. (A) Bug viewed under light microscopy; (B) bug excited by UV light, the externally visible fluorescence indicating the presence of rs on the membrane between the arms of the lb (arrowed). Dashed arrow indicates other areas of fluorescence on the abdomen that are not consistent between

specimens. rs whose presence is revealed by fluorescence on the metathorax is unlikely to participate in the snapping organ mechanism. lb, Y-lobe; rs, resilin; UV, ultraviolet. Image link.

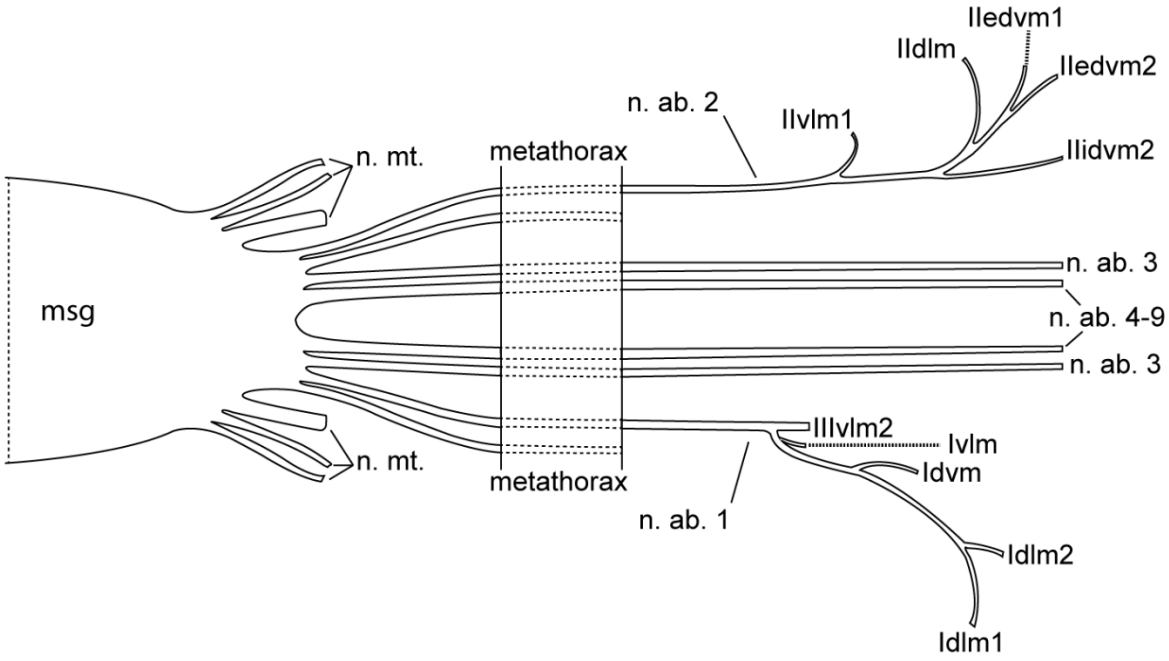

S2 Fig. Abdominal nervous system of a generalised planthopper. Nervous system reconstructed from SR-μCT of *A. bilobum* and an unidentified nogodinid and fulgorid (S1 Table), whose gross morphology of the nervous system was similar. The muscles of the second abdominal segment (top right) are innervated from the second abdominal nerve. Muscles from the first abdominal segment are innervated from their corresponding nerve. Innervation for muscles IIidvm1-IIisdvm could not be traced. idvm, internal dorsoventral muscle; isdvm, intersegmental dorsoventral muscle; msg, mesothoracic ganglion; n. ab. 1, abdominal nerve of segment 1; n. ab. 2, abdominal nerve of segment 2; n. ab. 3, abdominal nerve of segment three; n. ab. 4–9, abdominal nerve of segments four to nine; n. mt., metathoracic nerves; SR-μCT, synchrotron radiation microcomputed tomography. Image link.

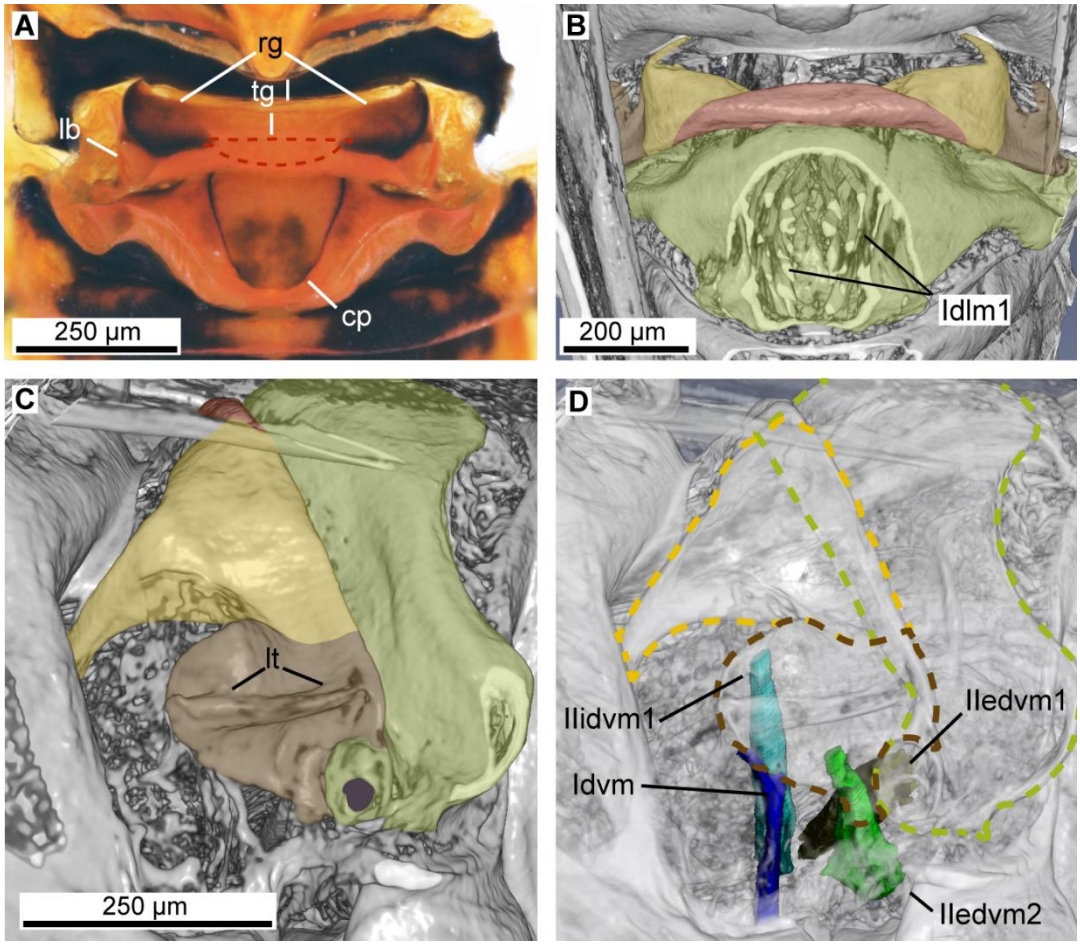

S3 Fig. Drumming organ of a generalized non-asiracine male delphacid, *S. minutus*. (A) Dorsal view of drumming organ in relaxed conformation in an ethanol-preserved specimen. (B) False-colour SR-µCT volume rendered image of the drumming organ. The top part of the organ is virtually sliced off, revealing the attachments of muscle Idlm1. (C) Lateral view of the drumming organ. (D) The same image, virtually made transparent to show the DVMs operating the drumming organ and their attachments. Dashed lines show the boundaries of the exoskeletal components of the drumming organ. Colour coding of structures: yellow = rg; brown = modified lb; green = tg2; pink = tg1. Tomographic data for this species are freely available at CXIDB: http://cxidb.org/id-93.html. cp, central plate; DLM, dorsal longitudinal muscle; DVM, dorsoventral muscle; lb, Y-lobe; lt, transverse list of modified Y-lobe; rg, ridge; SR-µCT, synchrotron radiation microcomputed tomography; tg1, tergum one; tg2, tergum 2. Image link.

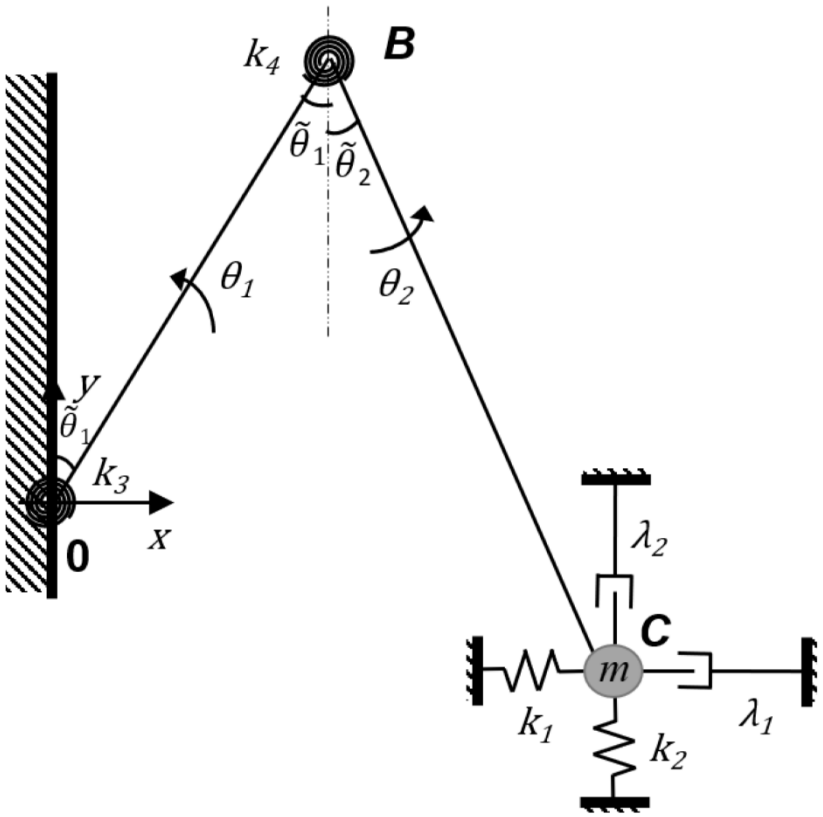

S4 Fig. Mathematical model of snapping organ. Two rigid bars articulate at points 0, B, and C, as dictated by torsion springs k3 and k4. The first rigid bar is attached to a fixed surface at 0, and a lumped mass (m) is attached to the second rigid bar at B. A system of linear springs and dampers connects to the mass at B. All parameters are measured from the real system (see S1 Methods), with the exception of k1, k2, λ1, and λ2, which were fitted by eye to match the measured motion (Fig 5). The model starts in the loaded state and then moves to the relaxed state; thus, unloading is modelled. Image link.

S5 Fig. Vibrometry recordings of vibration generation in a male *A. bilobum*, in which black, grey, and light grey represent recordings from the midabdomen, prothorax, and plant stem, respectively. Three repeats are plotted on each panel. (A) Time–velocity plots of recordings across multiple cycles, labelling the location of L and U phases over time. (B) Data from

panel A at higher temporal resolution for L, aligned in the time axis by the first peak maximum amplitude. (C) Data from panel A at higher temporal resolution for U, aligned in the time axis by the first peak maximum amplitude. Sample rates were 9.6 kHz, and all data are from the same individual. Data also shown in S1 Data, including attenuation calculations for minimum and maximum peaks during loading and unloading. L, loading; U, unloading. Image link.

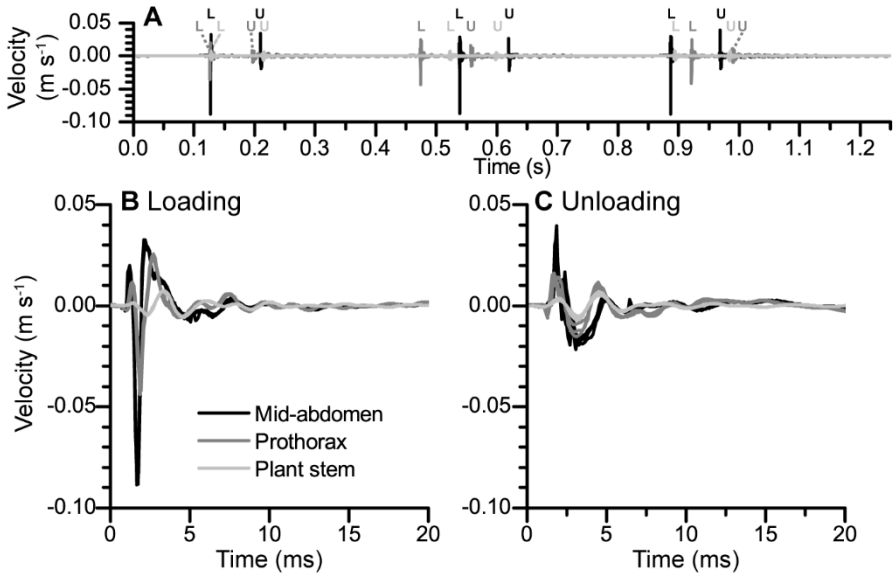

S1 Table. Species list of examined taxa, along with data on individual type of preservation, observation method, and depository. Examination of dry mounted specimens using microscopy only allowed documentation of exoskeletal morphology, while musculature was also studied in ethanol-preserved specimens. Use of SR-μCT permitted examination of the exoskeleton, musculature, and innervation of the snapping organ. Illustrations from the literature allowed examination of the external morphology of the vibrational organs of certain delphacids. The abovementioned observation methods allowed us to document the presence of a snapping organ (based on its defining characters) in all examined taxa, with the exception of non-Asiracinae delphacids, the latter having modified snapping organs. BMNH, Natural History Museum, London; DPC, Davranoglou Private Collection; MMBC, Moravian Museum, Brno; OUMNH, Oxford University Museum of Natural History; SR-μCT, synchrotron radiation microcomputed tomography; UG, University of Gdańsk. Table link.

Taxon	Preservation	Observation Method	Depository
Acanalonidae			

A. conica (Say, 1830)	Dry mounted	Microscopy	BMNH
A. servillei Spinola, 1839	Dry mounted	Microscopy	BMNH
A. sublinea (Walker, 1858)	Dry mounted	Microscopy	BMNH
Acanalonia sp. 1_Florida_OUMNH-2006-045	Dry mounted	Microscopy	OUMNH
Acanalonia sp. 2_Florida_OUMNH-2006-045	Dry mounted	Microscopy	OUMNH
Acanalonia sp. Belize_OUMNH-2002-006	Dry mounted	Microscopy	OUMNH
Acanalonia sp. Bolivia_OUMNH-2004-005	Dry mounted	Microscopy	OUMNH
Acanalonia sp. Argentina_OUMNH-2005-012	Dry mounted	Microscopy	OUMNH
Achilidae			
Achilus flammeus Kirby, 1818	Dry mounted	Microscopy	BMNH
Apateson albomaculatum Fowler, 1900	Dry mounted	Microscopy	MMBC
Cixidia skaloula (Asche, 2015)	ethanol; CPD	Microscopy; SR-μCT	DPC
Errada nebulosa (Distant, 1914)	Dry mounted	Microscopy	BMNH
Myconus collaris Melichar, 1904	Dry mounted	Microscopy	MMBC
Rhotala delineata Walker, 1857	Dry mounted	Microscopy	BMNH
Achilidae_Burmese_amber	Amber inclusion	SR-μCT	UG
Achilixiidae			
Achilixius bakeri Wilson, 1989	Dry mounted	Microscopy	BMNH
Bebaoiotes dorsivittata Fennah, 1947	Dry mounted	Microscopy	BMNH
Caliscelidae			
Bruchomorpha costaricensis Schmidt, 1927_OUMNH-2009-049	Ethanol	Microscopy	OUMNH
Caliscelis bonellii (Latreille, 1807)	ethanol; CPD	Microscopy; SR-μCT	DPC; BMNH
Peltonotellus quadrivittatus (Fieber, 1876)	Ethanol	Microscopy	DPC
Cixiidae			
Bothriocera westwoodi (Stal, 1856)	Dry mounted	Microscopy	MMBC

Cixiidae sp.1._ Mozambique_OUMNH-2010-098	ethanol; CPD	Microscopy; SR-μCT	OUMNH
Cixius sp.	Ethanol	Microscopy	DPC
Cixiidae sp.2._Mozambique_OUMNH-2010-098	ethanol; CPD	Microscopy; SR-μCT	OUMNH
Pentastira sp.	ethanol; CPD	Microscopy; SR-μCT	DPC
Pentastiridius leporinus (Linnaeus, 1761)	Dry mounted	Microscopy	MMBC
Tachycixius pilosus (Olivier, 1791)	Dry mounted	Microscopy	MMBC
Delphacidae			
Anakelisia perspicillata (Boheman, 1845)	image in publication [1]		
Asiraca clavicornis (Fabricius, 1794)	Ethanol	Microscopy	DPC; BMNH
Delphacidae sp._Mozambique_OUMNH-2010-098	ethanol; CPD	Microscopy; SR-μCT	OUMNH
Dicranotropis hamata (Boheman, 1847)	Ethanol	Microscopy	DPC; BMNH
Elaphodelphax nigropictus Fennah, 1949	image in publication [1]		
Kelisiinae sp._Greece	ethanol; CPD	Microscopy; SR-μCT	DPC
Liburnia britmusei Asche, 1983	image in publication [1]		
Neopunana saba Asche, 1983	image in publication [1]		
Stenocranus cf. minutus (Fabricius, 1787)	ethanol; CPD	Microscopy; SR-μCT	DPC
Derbidae			
Zoraidinae sp._Sulawesi_OUMNH-2010-089	ethanol; CPD	Microscopy; SR-μCT	OUMNH
Derbe pallida Fabricius, 1803	Dry mounted	Microscopy	MMBC
Malenia bosnica (Horvath, 1907)	Dry mounted	Microscopy	MMBC
Phenice signoreti (Coquerel, 1859)	Dry mounted	Microscopy	MMBC
Proutista moesta (Westwood, 1851)	Dry mounted	Microscopy	MMBC
Zoraida pterophoroides (Westwood, 1851)	Dry mounted	Microscopy	MMBC

Z. picta Distant, 1907	Dry mounted	Microscopy	MMBC
Dictyopharidae			
Bursinia genei (Dufur, 1849)	ethanol; CPD	Microscopy; SR-μCT	DPC; BMNH
Callodictya krueperi (Fieber, 1872)	Dry mounted	Microscopy	MMBC
Dictyophara europaea (Linnaeus, 1767)	ethanol; CPD	Microscopy; SR-μCT	DPC; BMNH
Orgeriinae sp.	ethanol; CPD	Microscopy; SR-μCT	DPC
Parorgerius platypus (Fieber, 1866)	Dry mounted	Microscopy	BMNH
Ranissus edirnaeus (Dlabola, 1957)	Dry mounted	Microscopy	MMBC
Eurybrachidae			
Aspidonitys trita Karsch, 1895	Dry mounted	Microscopy	BMNH
Chalia pulchra (Gray, 1832)	Dry mounted	Microscopy	OUMNH; BMNH
Mesonitys fuelleborni Schmidt, 1908	Dry mounted	Microscopy	OUMNH; BMNH
M. taeniata (Schmidt, 1906)	Dry mounted	Microscopy	BMNH
Platybrachys barbata (Fabricius, 1775)	Dry mounted	Microscopy	BMNH
P. leucostigma (Walker, 1851)	Dry mounted	Microscopy	BMNH
Flatidae			
Flatidae sp._Mozambique_OUMNH-2010-098	ethanol; CPD	Microscopy; SR-μCT	OUMNH
Hansenia pulverulenta (Guerin-Meneville, 1844)	Dry mounted	Microscopy	MMBC
Ityraea nigrocincta (Walker, 1858)_ OUMNH-1918-005	Dry mounted	Microscopy	OUMNH
Metcalfa pruinosa (Say, 1830)	Dry mounted	Microscopy	MMBC
Phantia subquadrata (Herrich-Schaeffer, 1838)	ethanol; CPD	Microscopy; SR-μCT	DPC; MMBC
Poeciloptera phalaenoides (Linnaeus, 1758)	Dry mounted	Microscopy	MMBC
Fulgoridae			
Aphaena aurantia (Hope, 1840)_ OUMNH-2019-005	Dry mounted	Microscopy	OUMNH
Aracynthus sanguineus (Olivier, 1791)	Dry mounted	Microscopy	MMBC

Cornelia nympha Stal, 1866	Dry mounted	Microscopy	MMBC
Diareusa imitatrix Ossiannilsson, 1940_OUMNH-2004-005	Dry mounted	Microscopy	OUMNH
Eddara euchroma Walker, 1858	Dry mounted	Microscopy	MMBC
Fulgoridae sp._Mozambique_OUMNH-2010-098	ethanol; CPD	Microscopy; SR-μCT	OUMNH
Kasserota pupillata (Stal, 1863)	Dry mounted	Microscopy	MMBC
Laternaria phosphorea (Linnaeus, 1764)	Dry mounted	Microscopy	MMBC
Loxocephala decora (Walker, 1851)	Dry mounted	Microscopy	MMBC
Phenax variegata (Olivier, 1791)_ OUMNH-2019-006	Dry mounted	Microscopy	OUMNH
Phrictus quinquepartitus Distant, 1883	Dry mounted	Microscopy	MMBC
Pyrops sultana (Adams & White, 1847)_OUMNH-2011-043	Dry mounted	Microscopy	OUMNH
Saiva transversolineata (Baker, 1925)	Dry mounted	Microscopy	MMBC
Gengidae			
Gengis panoblites Fennah, 1949	Dry mounted	Microscopy	BMNH
Hypochthonellidae			
Hypochthonella caeca China & Fennah, 1952	Dry mounted	Microscopy	BMNH
Issidae			
Agalmatium bilobum (Fieber, 1877)	ethanol; CPD	Microscopy; SR-μCT	DPC; BMNH
Atylana herbida (Walker, 1870)	Dry mounted	Microscopy	BMNH
Falcidius apterus (Fabricius, 1794)	Dry mounted	Microscopy	MMBC
Forculus peculiaris Distant, 1912	Dry mounted	Microscopy	BMNH
Gergithus niger (Walker, 1857)	Dry mounted	Microscopy	MMBC
Glyphotonga acuminata Schmidt, 1910	Dry mounted	Microscopy	BMNH
Hemisphaerius coccineloides (Burmeister, 1834)	Dry mounted	Microscopy	MMBC
Hemispharinae_sp._Mozambique_OUMNH-2010-098	ethanol; CPD	Microscopy; SR-μCT	OUMNH
Issidae sp. Sabah_OUMNH-2013-056	Ethanol	Microscopy	OUMNH
Latematium graecicum (Dlabola, 1982)	Ethanol	Microscopy	DPC
Mycterodus pallens Stal, 1861	ethanol; CPD	Microscopy; SR-μCT	DPC

Oryxana subacuta (Walker, 1870)	Dry mounted	Microscopy	BMNH
Thabenoides opalina (Distant, 1916)	Dry mounted	Microscopy	BMNH
Tonga foliacea (Stal, 1859)	Dry mounted	Microscopy	BMNH
T. guttulata (Westwood, 1845)	Dry mounted	Microscopy	BMNH
Kinnaridae			
Kinnara ceylonica (Melichar, 1903)	Dry mounted	Microscopy	MMBC
K. flavofasciata Distant, 1916	Dry mounted	Microscopy	BMNH
Nesomicrixia insularis (Synave, 1958)	Dry mounted	Microscopy	BMNH
Lophopidae			
Elasmoscelis sp._Mozambique_OUMNH-2010-098	ethanol; CPD	Microscopy; SR-μCT	OUMNH
Meenoplidae			
Anigrus bergrothi (Muir, 1927)	Dry mounted	Microscopy	BMNH
Meenoplidae sp.Sabah_OUMNH-2013-056	Ethanol	Microscopy	OUMNH
Meenoplidae sp._Mozambique_OUMNH-2010-098	Ethanol	Microscopy	OUMNH
Meenoplus albosignatus Fieber, 1866	Dry mounted	Microscopy	MMBC
Phaconeura fletcheri Kirkaldy, 1908	Dry mounted	Microscopy	BMNH
Nogodinidae			
Biolleyana fenestra (Gerstaecker, 1895)	Dry mounted	Microscopy	MMBC
Indogaetulia nigrovenosa (Melichar, 1898)	Dry mounted	Microscopy	BMNH
Mindura simiana Distant, 1910	Dry mounted	Microscopy	BMNH
Monteira cornicula Melichar, 1906	Dry mounted	Microscopy	BMNH
Nogodinidae sp._Mozambique_OUMNH-2010-098	ethanol; CPD	Microscopy; SR-μCT	OUMNH
Nogodinidae sp. Honduras	Ethanol	Microscopy	DPC
Psiadiicola brevipennis Fennah, 1978	Dry mounted	Microscopy	BMNH
Sassula concolor (Walker, 1870)	Dry mounted	Microscopy	BMNH
Varcia greeni (Kirby, 1891)	Dry mounted	Microscopy	MMBC
V. pyramidalis Melichar, 1898	Dry mounted	Microscopy	MMBC
Ricaniidae			
Pocharista conradti (Schmidt, 1906)	Dry mounted	Microscopy	MMBC

Pochazia flavocostata Melichar, 1898	Dry mounted	Microscopy	MMBC
Ricania discoptera Stal, 1865	Dry mounted	Microscopy	MMBC
R. trimaculata Guerin-Meneville, 1838	Dry mounted	Microscopy	MMBC
Ricanoptera mellerborgi (Lallemand, 1854)	Dry mounted	Microscopy	MMBC
Tettigometridae			
Euphyonarthex sp._Cameroon_OUMNH-2019-004	Dry mounted	Microscopy	OUMNH
Tettigometra atra Hagenbach, 1825	Dry mounted	Microscopy	MMBC
T. impressifrons Mulsant & Rey, 1855	Ethanol	Microscopy	DPC
T. laeta Herrich-Schaeffer, 1835	ethanol; CPD	Microscopy; SR-μCT	DPC
T. leucophaea (Preyssler, 1792)	Dry mounted	Microscopy	MMBC
Tropiduchidae			
Cixiopsis punctatus Matsumura, 1900	Dry mounted	Microscopy	BMNH
Eilithyia insularis Distant, 1912	Dry mounted	Microscopy	BMNH
Epora montana Distant, 1912	Dry mounted	Microscopy	BMNH
Eporiella ceylonica Melichar, 1914	Dry mounted	Microscopy	BMNH
Isporisa apicalis Walker, 1857	Dry mounted	Microscopy	BMNH
Leusaba marginalis Walker, 1857	Dry mounted	Microscopy	BMNH
Ommatissus binotatus Fieber, 1876	Dry mounted	Microscopy	MMBC
Padanda denti Muir, 1934	Dry mounted	Microscopy	BMNH
Paricana dilatipennis Walker, 1857	Dry mounted	Microscopy	BMNH
Pseudoclardea leguati (Muir, 1925)	Dry mounted	Microscopy	BMNH
Stacota breviceps (Walker, 1858)	Dry mounted	Microscopy	BMNH
Trypetimorpha fenestrata Costa, 1862	Dry mounted	Microscopy	MMBC
Tropiduchidae sp.Sabah_OUMNH-2013-056	Ethanol	Microscopy	OUMNH
Vanua respicienda (Walker, 1858)	Dry mounted	Microscopy	BMNH
Varma tridens Distant, 1906	Dry mounted	Microscopy	BMNH

Reference

1. Asche M. Zur phylogenie der Delphacidae Leach, 1815 (Homoptera Cicadina Fulgoromorpha). Marburg Entomol Publ. 1985; 2: 1-398.

S2 Table. Muscles operating the snapping organ of Fulgoromorpha, based on dissection of ethanol-preserved specimens and SR-μCT scans. Function of muscles was inferred by high-speed videography, power calculations of laser Doppler vibrometry recordings of A. bilobum, and artificial contraction of the respective muscles using a pair of forceps in ethanol-preserved specimens. SR-μCT, synchrotron radiation microcomputed tomography. Table link.

Muscle	Origin	Insertion	Inferred function
Idlm1	Apodeme on metaphragma	Apodeme of tergum two	Raises the abdomen; acts a spring, storing and releasing energy during loading phase
Idlm2	Strip of tergum one	Tergum two	Assists in closure of Y-lobe arms
Idvm	Postcoxale	Base of Y-lobe, immediately above connector, beneath vertical list	Pulls Y-lobe downward
IIedvm1	Apical third of stnIIa	Proximal portion of spine-like apodeme of tergum two	Moves spine-like apodeme (and as a result base of Y-lobe as well) downward, causing closure of Y-lobe arms during loading phase
IIedvm2	Apex of stnIIa	Distal portion of spine-like apodeme of tergum two	Moves spine-like apodeme (and as a result base of Y-lobe as well) downward, causing closure of Y-lobe arms during loading phase
IIidvm1	Small apodeme on median region of stnnIIa	Membrane immediately anterior to base of Y-lobe	Unknown
IIidvm2	Apical third of stnIIa, slightly lower than IIedvm2	Connector arm of tergum two	Assists in closure of Y-lobe arms
IIisdvm	Apex of stnIIb	Anterior margin of tergum three	Unknown
IIIvlm2	Metafurca	Antecosta of segment 1	Moves abdomen downward
Ivlm	Base of postcoxale	Antecosta of segment 1	Assists in moving abdomen downward
IIvlm1	Sternum IIa	Sternum IIb	Contraction of Sternum IIa-b

S3 Table. List of previous names for planthopper muscles (all delphacids), homologised with the terminology applied in the present study for the snapping organ musculature. Inferences of homology and segmental identity were based on muscle innervation and location from SR-μCT and ethanol-preserved specimens. En-dash (–) denotes that the character is either absent or not reported by the study in question. SR-μCT, synchrotron radiation microcomputed tomography. Table link.

Taxon:	***Dicranotropis hamata* (Boheman, 1847)**	***Nilaparvata lugens* (Stal, 1854)**	***Stenocranus fuscovittatus* (Stal, 1858)**
Muscle			
Idlm1	Iadlm1	DLM1	Iadlm1
Idlm2	Iadlm2	DLM2	-
IIIvlm2	IIIvlm	VLM1	-
Ivlm1	-	-	-
IIvlm1	Iavlm1	VLM4	-
IIvlm2	Iavlm2	VLM2	Iavlm2
IIvlm3	-	VLM3	-
Idvm1	-	-	-
IIidvm1	Iadvm1	DVM1	Iadvm1
IIidvm2	-	-	-
IIedvm1	Iadvm2	DVM 2	Iadvm2
IIedvm2	Iadvm3	DVM 3	-
IIisdvm	-	ISM1	-
Author:	[1]	[2]	[3]

References

1. Ossiannilsson F. Insect drummers. A study on the morphology and function of the sound-producing organ of swedish Homoptera Auchenorrhyncha. Op Ent Suppl 10. 1949; 3: 1-146.

2. Mitomi M, Ichikawa T & Okamoto H. Morphology of the vibration-producing organ in adult rice brown planthopper, *Nilaparvata lugens* (Stal) (Homoptera: Delphacidae). Appl Entomol Zool. 1984; 19: 407-417.

3. Asche M. Zur phylogenie der Delphacidae Leach, 1815 (Homoptera Cicadina Fulgoromorpha). Marburg Entomol Publ. 1985; 2: 1-398.

S4 Table. Character states representing major transformations of the snapping organ in Fulgoromorpha. Characters of delphacids largely based on the meta-analysis of Asche, 1990 [34] and our own observations of ethanol-preserved and SR-µCT specimens. Order of character states does not imply evolutionary sequence. SR-µCT, synchrotron radiation microcomputed tomography. Table link.

Character number	Character state
Non-Asiracinae Delphacidae	
1	Snapping organ sexually dimorphic
2	Ventrocaudal enlargement of Idlm1-bearing apodemes and migration to median region of metapostnotum
3	Enlargement of dorsoventral musculature and IIvlm2
4	Fusion and modification of Y-lobe
5	Enlarged sternal apodemes for IIvlm2
6	Detachment of spiracle lobe from tergum two and partial fusion to Y-lobe
7	Development of central plate on tergum two
Derbidae (non-Cedusinae)	
8	Y-lobe externally obscure, extremely flat, covered by ridge and membranes
9	Metathoracic wing stridulatory device

S1 Data (Excel file link)

Three tabs show (i) vibrometry data from the midabdomen during loading and unloading (three measurements from individual 1), along with calculations of peak coordinates, time since x-axis crossing, and attenuation of peak motions from midabdomen to plant substrate and prothorax to plant substrate; (ii) vibrometry data from the laser focussed on plant substrate (individual 1), prothorax (individual 1), and bug genitalia (individual 2) during loading and unloading; and (iii) power calculations.

S1 Movie (MP4 file link)

High-speed camera recordings (100 frames per second) of the snapping organ of a male *A. bilobum* in action. 0–10 s, lateral view; 10–15 s, caudal view; 15–20 s, dorsal view.

Chapter 4: On the morphology and possible function of two putative vibroacoustic mechanisms in derbid planthoppers (Hemiptera: Fulgoromorpha: Derbidae)

Leonidas-Romanos Davranoglou[1], Beth Mortimer[1], Graham K. Taylor[1], Igor Malenovský[2]

[1]Department of Zoology, University of Oxford, Oxford OX1 3PS, U.K.;

[2]Department of Botany and Zoology, Faculty of Science, Masaryk University, Kotlářská 2, Brno, CZ-611 37, Czech Republic

Supplementary material

S1 Table (Excel file link)

Distribution of stridulatory mechanisms and snapping organs in derbid planthoppers. All observations were made on dry-mounted specimens, using light stereomicroscopy. Hyphen (-) denotes that the said structure could not be observed in the particular specimen. The absence or presence of a certain structure is specifically stated. Abbreviations for depositories: Natural History Museum of London (BMNH); Moravian Museum of Brno (MMBC).

Chapter 6: On the morphology and evolution of cicadomorphan tymbal organs

Supplementary Material

Figure S1. Detail of the right tymbal and ribs of a male *Aphrophora alni* (Fallén, 1805).

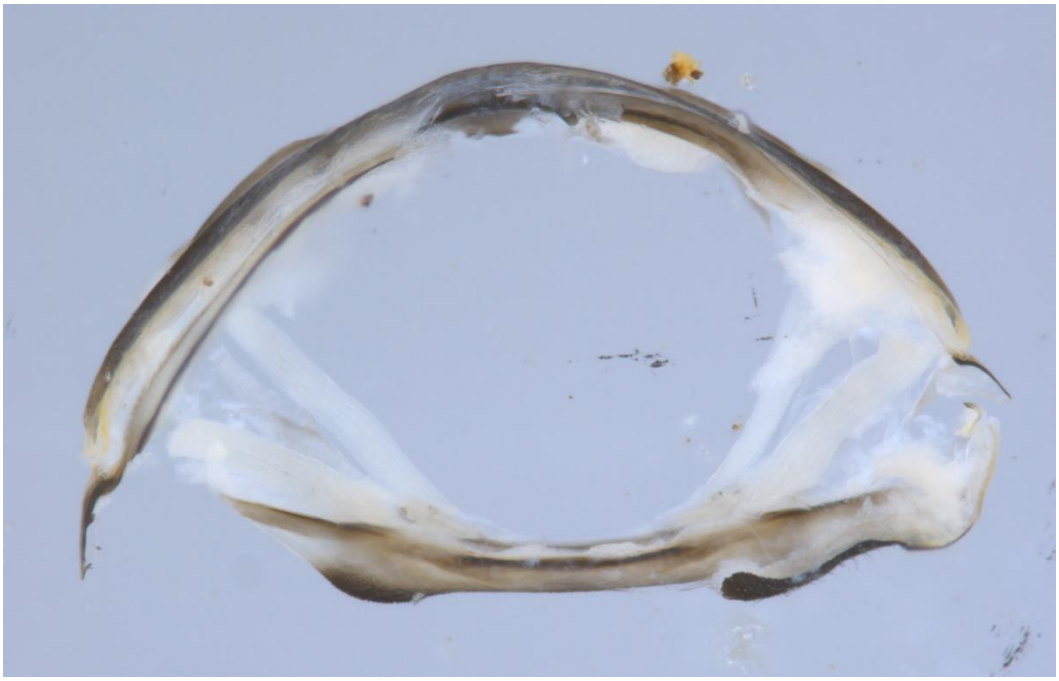

Figure S2. Caudal view of a cross-section of the tymbal and tymbal muscles of a female *Philaenus spumarius* (Linnaeus, 1758).

Figure S3. Longitudinal dissection of *Tibicen plebejus* (Scopoli, 1763), showing the enlarged tymbal muscles.

Figure S4. Dorsal view of pregenital abdomen and tymbal lobes of a female *Evacanthus interruptus* (Linnaeus, 1758).